Origins of Stereocontrol in the [2 + 2] Cycloaddition between Achiral Ketenes and Chiral α-Alkoxy Aldehydes. A Pericyclic Alternative to the Aldol Reaction

Begoña Lecea, Ana Arrieta, Iosune Arrastia, and Fernando P. Cossío*

Kimika Fakultatea, Euskal Herriko Unibertsitatea, P.K. 1072, San Sebastián-Donostia, Spain, and Farmazi Fakultatea, Euskal Herriko Unibertsitatea, P.K. 450, 010080 Vitoria-Gasteiz, Spain

Received April 8, 1998

Ab Initio calculations predict that the thermal [2 + 2] cycloaddition reaction between C_{2v}-symmetric ketenes and enantiopure aldehydes takes place with high enough stereocontrol for preparative purposes. The sense of induction is predicted to be non-Felkin. It is also found that the [2 + 2] cycloaddition involving nonactivated ketenes is facilitated by using 5 M solutions of lithium perchlorate in diethyl ether. It is found that both the purely thermal and lithium-assisted [2 + 2] cycloadditions result in the same type of stereocontrol. This method constitutes a general route for the synthesis of homochiral 2-oxetanones and related compounds, thus providing a pericyclic alternative to the aldol reaction.

Introduction

Since the pioneering studies of Wilsmore and Staudinger,[1] the exceptional ability of ketenes to participate in thermal cycloadditions is well recognized. Indeed, in his recent monograph on ketenes,[2] Tidwell has written that "cycloaddition has remained as the most distinctive, useful, and intellectually challenging, aspect of ketene chemistry." In particular, these heterocumulenes are very versatile reagents for thermal [2 + 2] cycloadditions.[2,3] Given that this kind of reaction is in general difficult under thermal conditions, the electronic peculiarities of ketenes attracted considerable attention in the course of the development of the theory of pericyclic reactions.[4] Therefore, [2 + 2] cycloadditions between ketenes and imines,[5] alkenes,[6] alkynes,[7] nitroso,[8] azo,[9] and carbonyl[10] compounds have been described, and some of these reactions have proven to be very useful in the chemical synthesis of pharmacologically valuable compounds.[11]

Although all the above-mentioned reactions can be formally envisaged as [2 + 2] cycloadditions, the actual mechanisms operating in these transformations can be different. This variable behavior can be rationalized by taking into account that the π-frontier orbitals of ketenes lie in orthogonal planes.[2] Thus, a nucleophile can interact with the ipso sp-hybridized carbon atom of the ketene by means of the in-plane interaction depicted in Figure 1. On the other hand, an electrophile must interact via the α carbon atom of the ketene. The trajectory of this latter attack is determined by the HOMO plane of the ketene, which is perpendicular to its molecular plane (Figure 1).

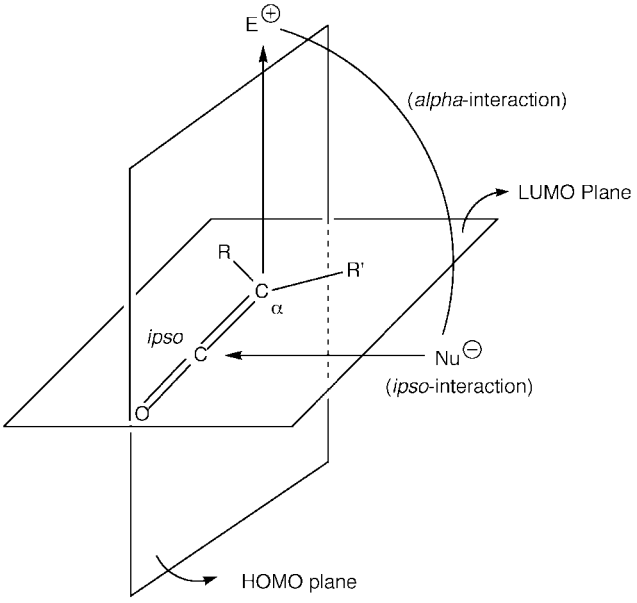

Figure 1. Schematic representation of the reactive sites of a ketene toward nucleophiles (ipso interaction) and electrophiles (α interaction). The curved line represents an intramolecular connection between the nucleophilic and electrophilic sites.

In a concerted reaction, the ketene and the π-system must suffer both interactions in a single—but not necessarily synchronous—step, thus leading to a distorted nonsupra-supra geometry of the corresponding transition state, such as the $[_{\pi}2_s + _{\pi}2_a]$ mechanism proposed by

(1) (a) Wilsmore, N. T. M. *J. Chem. Soc.* **1907**, *91*, 1938. (b) Staudinger, H.; Kleuer, H. W. *Chem. Ber.* **1906**, *39*, 968.
(2) Tidwell, T. T. *Ketenes*; Wiley: New York, 1995; pp 459−571 and references therein.
(3) (a) Hyatt, J. A.; Raynolds, P. W. Ketene Cycloadditions. In *Organic Reactions*; Paquette, L., et al., Eds.; Wiley: New York, 1994; Vol. 45, pp 159−646. (b) Ghosez, L.; Marchand Brynaert, J. In *Comprehensive Organic Chemistry*; Trost, B. M., Fleming, I., Eds.; Pergamon: Oxford, 1991; Vol. 5, pp 86−89. (c) Oligaruso, M. A.; Wolfe, J. F. In *Synthesis of Lactones and Lactams*; Patai, S., Rappoport, Z., Eds.; Wiley: Chichester, 1993; pp 63−76, 303.
(4) Wang, X.; Houk, K. N. *J. Am. Chem. Soc.* **1990**, *112*, 1754 and footnote 10 therein.
(5) Georg, G. I.; Ravikumar, V. T. In *The Organic Chemistry of β-Lactams*; Georg, G.-L., Ed.; Werlag Chemie: New York, 1993; pp 295−331.
(6) Snider, B. B. *Chem. Rev.* **1988**, *88*, 793.
(7) See, for example: (a) Hassner, A.; Dillon, J. *Synthesis* **1979**, 689. (b) Danheiser, R. L.; Savariar, S. *Tetrahedron Lett.* **1987**, *28*, 3299. (c) Fishbein, P. L.; Moore, H. W. *J. Org. Chem.* **1985**, *50*, 3226.
(8) (a) Kerber, R. C.; Cann, M. C. *J. Org. Chem.* **1974**, *39*, 2552. (b) Kresze, G.; Trede, A. *Tetrahedron* **1963**, *19*, 133.
(9) (a) Fahar, E.; Fisher, W.; Jung, A.; Savel, L. *Tetrahedron Lett.* **1967**, 161. (b) Hall, J. H.; Kellogg, R. M. *J. Org. Chem.* **1966**, *31*, 1079.
(10) Pommier, A.; Pons, J.-M. *Synthesis* **1993**, 441.
(11) Pommier, A.; Pons, J.-M. *Synthesis* **1995**, 729.

S0022-3263(98)00651-3 CCC: $15.00 © 1998 American Chemical Society
Published on Web 07/08/1998

Scheme 1[a]

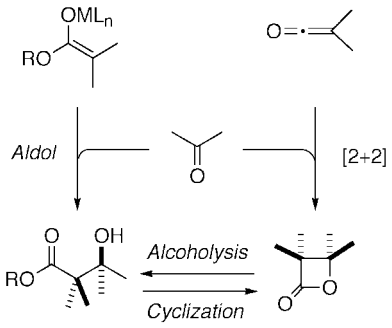

[a] The possible substituents at the different positions are not specified.

Woodward and Hoffmann[12] or, more recently the [$_\pi2_s$ + ($_\pi2_s$ + $_\pi2_s$)] mechanism.[13]

According to the above-mentioned scheme, electrophilic ketenes, namely those incorporating electron-withdrawing groups, will be especially prone to the ipso interaction represented in Scheme 1. If the other partner is in turn nucleophilic enough, the relative importance of the ipso interaction is quite large and the cycloaddition is actually a two-step reaction in which the $C_{ipso}-Y$ bond is formed first, followed by a ring closure to form the $C_\alpha-X$ bond. This is the case in the reaction between ketenes and imines, also known as the Staudinger reaction. This nonconcerted mechanism has been studied by our group[14] and by others.[15] In other cycloadditions, the interaction between ketenes and π-systems is concerted, although quite asynchronous. In general, the $C_\alpha-X$ interaction is developed to a lesser extent.

Recently, we have published two papers concerning the thermal [2 + 2] cycloaddition between ketenes and carbonyl compounds.[16] This reaction has also been explored computationally by Rajzmann[17] and Yamabe.[18] It has been found that this reaction is concerted and follows a [$_\pi2_s$ + ($_\pi2_s$ + $_\pi2_s$)] mechanism in the absence of Lewis acid catalysts. The preparative potential of this reaction has been explored by different groups.[10,11] This is not surprising since the reaction can be considered as a "pericyclic" alternative to the aldol reaction, the latter being of paramount importance in organic synthesis.[19] In effect, the product of this [2 + 2] cycloaddition, namely a 2-oxetanone (β-lactone), and the product of an aldol reaction, for instance, a β-hydroxy ester, can be interconverted into each other via alcoholysis or cyclization, respectively (Scheme 1). However, two drawbacks have hampered the development of this reaction: First, in general, nonnucleophilic ketenes are quite unreactive toward carbonyl compounds unless suitable catalysts are employed.[3,11] Second, the stereoselectivity of the cycloaddition is in general poor, although efficient stereocontrol for the catalyzed version has been achieved in several cases.[3,11,20]

Within this context, the aim of the present work has been to explore computationally the possibility of achieving high stereocontrol in the [2 + 2] cycloaddition between C_{2v}-symmetric ketenes and homochiral aldehydes. In addition, since we have developed recently[21] a method that allows the [2 + 2] cycloaddition between unactivated ketenes and aromatic or α,β-unsaturated aldehydes, we have verified the predictions made by theoretical methods. The final goal of the work has been to improve our understanding of the reasons underlying the stereocontrol in this kind of cycloadditions, thus yielding a complementary alternative to aldol-type reactions.

Computational Methods

All ab initio calculations described in this work have been carried out using the GAUSSIAN 94[22] suite of programs. The 6-31G* basis set[23] was used, and the geometries of all the stationary points were fully optimized using analytical gradient techniques.[24]

Most of the saddle points were located and optimized using the eigenvector-following algorithm.[25] In these cases, the possible conformers were explored at the HF/6-31G* and HF/AM1[26] levels. The conformer distribution of the diastereomeric cycloadducts was explored by means of Monte Carlo simulations[27] using the MM2* force field[28]

(12) Woodward, R. B.; Hoffmann, R. *The Conservation of Orbital Symmetry*; Verlag Chemie−Academic Press: New York, 1970; p 163.
(13) (a) Pasto, D. J. *J. Am. Chem. Soc.* **1979**, *101*, 37. (b) Valentí, E.; Pericàs, M. A.; Moyano, A. *J. Org. Chem.* **1990**, *55*, 3582. (c) Krabbenhoft, H. O. *J. Org. Chem.* **1978**, *43*, 1305.
(14) (a) Cossío, F. P.; Ugalde, J. M.; Lopez, X.; Lecea, B.; Palomo, C. *J. Am. Chem. Soc.* **1993**, *115*, 995. (b) Cossío, F. P.; Arrieta, A.; Lecea, B.; Ugalde, J. M. *J. Am. Chem. Soc.* **1994**, *116*, 2085. (c) Arrieta, A.; Ugalde, J. M.; Cossío, F. P.; Lecea, B. *Tetrahedron Lett.* **1994**, *35*, 4465. (d) Arrastia, I.; Arrieta, A.; Ugalde, J. M.; Cossío, F. P.; Lecea, B. *Tetrahedron Lett.* **1994**, *35*, 7825. (e) Lecea, B.; Arrastia, I.; Arrieta, A.; Roa, G.; Lopez, X.; Arriortua, M. I.; Ugalde, J. M.; Cossío, F. P. *J. Org. Chem.* **1996**, *61*, 3070.
(15) (a) Sordo, J. A.; González, J.; Sordo, T. L. *J. Am. Chem. Soc.* **1992**, *114*, 6249. (b) López, R.; Sordo, T. L.; Sordo, J. A.; González, J. *J. Org. Chem.* **1993**, *58*, 7036. (c) Assfeld, X.; Ruiz-López, M. F.; González, J.; López, R.; Sordo, J. A.; Sordo, T. L. *J. Comput. Chem.* **1994**, *15*, 479. (d) López, R.; Ruiz-López. M. F.; Rinaldi, D.; Sordo, J. A.; Sordo, T. L. *J. Phys. Chem.* **1996**, *100*, 10600. (e) Boyd, D. B. Computer-Assisted Molecular Design Studies of β-Lactam Antibiotics. In *Frontiers on Antibiotic Research*; Umezawa, H., Ed.; Academic Press: Tokyo, 1987; pp 339−356. (f) Cooper, R. D. G.; Daugherty, B. W.; Boyd, D. B. *Pure Appl. Chem.* **1987**, *59*, 485.
(16) (a) Lecea, B.; Arrieta, A.; Roa, G.; Ugalde, J. M.; Cossío, F. P. *J. Am. Chem. Soc.* **1994**, *116*, 9613. (b) Lecea, B.; Arrieta, A.; Lopez, X.; Ugalde, J. M.; Cossío, F. P. *J. Am. Chem. Soc.* **1995**, *117*, 12314.
(17) (a) Pons, J.-M.; Pommier, A.; Rajzmann, M.; Liotard, D. *THEOCHEM* **1994**, *313*, 361. (b) Pons, J.-M.; Oblin, M.; Pommier, A.; Rajzmann, M.; Liotard, D. *J. Am. Chem. Soc.* **1997**, *119*, 3333.
(18) Yamabe, S.; Minato, T.; Osamura, Y. *J. Chem. Soc., Chem. Commun.* **1993**, 450.
(19) See, for example: (a) Evans, D. A.; Nelson, J. V.; Taber, T. R. *Top. Stereochem.* **1982**, *13*, 1. (b) Kaiama, T.; Kobayashi, S. In *Organic Reactions*; Paquette, L., et al., Eds.; Wiley: New York, 1994; Vol. 46.
(20) (a) Pommier, A.; Pons, J.-M.; Kocienski, P. J. *J. Org. Chem.* **1995**, *60*, 7334. (b) Pommier, A.; Pons, J.-M.; Kocienski, P. J.; Wong, L. *Synthesis* **1995**, 1294. (c) Song, C. E.; Ryu, T. H. R.; Roh, E. J.; Kim, I. O.; Ha, H.-J. *Tetrahedron: Asymmetry* **1994**, *5*, 1215. (d) Tamai, Y.; Yoshiwara, H.; Someya, M.; Fukumoto, J.; Miyano, S. *J. Chem. Soc., Chem. Commun.* **1994**, 2281. (e) Palomo, C.; Miranda, J. I.; Cuevas, C.; Odriozola, J. M. *J. Chem. Soc., Chem. Commun.* **1995**, 1735. (f) Tamai, Y.; Someya, M.; Fukumoto, J.: Miyano, S. *J. Chem. Soc., Perkin Trans. 1* **1994**, 1549.
(21) Arrastia, I.; Cossío, F. P. *Tetrahedron Lett.* **1996**, *37*, 7143.
(22) GAUSSIAN 94, Revision B.2: Frisch, M. J.; Trucks, G. W.; Schlegel, H. B.; Gill, P. M. W.; Johnson, B. G.; Robbb, M. A.; Cheeseman, J. R.; Keith, T.; Peterson, G. A.; Montgomery, J. A.; Raghavachari, K.; Al-Laham, M. A.; Zakrzewski, V. G.; Ortiz, J. V.; Foresman, J. B.; Peng, C. Y.; Ayala, P. Y.; Chen, W.; Wong, M. W., Andres, J. L.; Replogle, E. S.; Gomperts, R.; Martin, R. L.; Fox, D. J.; Binkley, J. S.; Defrees, D. J.; Baker, J.; Stewart, J. P.; Head-Gordon, M.; Gonzalez, C.; Pople, J. A. Gaussian, Inc., Pittsburgh, PA, 1995.
(23) Hehre, W. J.; Radom, L.; Schleyer, P.v. R.; Pople, J. A. *Ab Initio Molecular Orbital Theory*; Wiley: New York, 1986; p 82 and references therein.
(24) See ref 23, pp 55, 56 and references therein.
(25) Baker, J. *J. Comput. Chem.* **1986**, *7*, 385.
(26) Dewar, M. J. S.; Zoebish, E. G.; Healy, E. F.; Stewart, J. J. P. *J. Am. Chem. Soc.* **1985**, *107*, 3902.
(27) (a) Chang, G.; Guida, W. C.; Still, W. C. *J. Am. Chem. Soc.* **1989**, *111*, 4379. (b) Saunders: M.; Houk, K. N.; Wu, Y.-D.; Still, W. C.; Lipton, M.; Chang, G.; Guida, W. *J. Am. Chem. Soc.* **1990**, *112*, 1419.
(28) Allinger, N. L. *J. Am. Chem. Soc.* **1977**, *99*, 8127.

as implemented in the Macro Model package.[29] The selected minima were further reoptimized at the RHF/AM1 and HF/6-31G* levels. Unless otherwise stated, conformers included in the next section represent the lowest energy conformation for a given reaction path.

All the saddle points located and characterized at the HF/6-31G* level were further optimized using density functional theory[30] (DFT). For this purpose, we have used the hybrid three-parameter functional developed by Becke,[31] which has proven to be quite reliable in pericyclic reactions.[32] This functional combines the Becke's gradient corrected functional and the Lee−Yang−Parr and Vosko−Wilk−Nusair correlation functionals[31] with part of the exact Hartree−Fock exchange energy. This method is denoted in the text as B3LYP. All stationary points were characterized by harmonic analysis.[33] Zero-point energies obtained at the HF/6-31G* levels were scaled[34] by a factor of 0.89. The ZPVEs obtained at the B3LYP/6-31G* level were not scaled.

The differences in energy were computed at the B3LYP/6-31G* level, including ZPVE corrections. Aside from the DFT calculations, electron correlation has been also estimated at the second-order Møller−Plesset (MP2)[35] level on HF/6-31G* geometries.

Given the importance of solvent effects in cycloaddition reactions,[36] several calculations were also performed taking into account these effects. Solvent effects were considered using the self-consistent reaction field (SCRF) method.[37] In one of the SCRF methods included in our calculations, the solute is described by its dipole moment and an spherical cavity of radius a_o. The solvent is described by its dielectric constant ϵ. This method is usually mentioned as the Onsager model.[38] In this work, it will be denoted as L1A1 (multipole expansion truncated at $l_{max} = 1$, spherical cavity).[38] In a previous paper,[39] we have found that the description provided by the L1A1 model is not accurate enough for describing diastereomeric structures in which the relative orientation of the dipoles can promote substantial variations in the quadrupole and higher multipoles. Therefore, we have also calculated the relative energies of several stationary points using the SCIPCM model.[40] This approach can be considered as equivalent to an infinite expansion in the multipole series. Most of the calculations included in this work have been computed at $\epsilon = 9.08$, which corresponds to dichloromethane.

Donor−acceptor interactions have been calculated by means of the natural bond orbital (NBO) model.[41] According to the NBO decomposition, the energy of a donor−acceptor interaction is given by

$$\Delta E^{(2)}_{\phi\phi^*} = -n_\phi \frac{\langle \phi^* | \hat{F} | \phi \rangle^2}{\epsilon_{\phi^*} - \epsilon_\phi} \qquad (1)$$

where n_ϕ is the occupation number of the donor orbital, $\hat{F}$ is the Fock operator, ϕ and ϕ^* are two filled and unfilled NBOs, respectively, and ϵ_ϕ and ϵ^*_ϕ are their respective energies. The Wiberg bond indices[42] have also been computed on an NBO basis.

Scheme 2

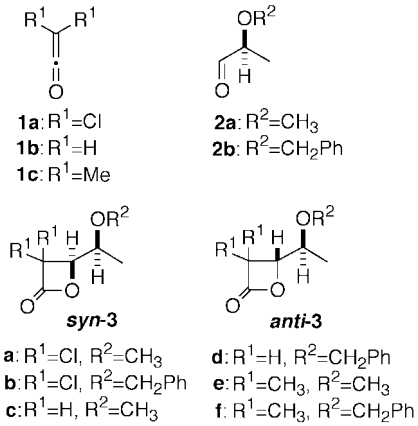

Results and Discussion

As representative model compounds, we selected the ketenes and aldehydes shown in Scheme 2. Apart from ketene **1b** itself, we have selected dichloroketene **1a** as a model of an activated electrophilic ketene and dimethylketene **1c** as a representative case of a stabilized nonelectrophilic ketene.[43] (*S*)-2-Methoxypropionaldehyde **2a** was considered as a computationally tractable analogue of the synthetically more useful (*S*)-2-(benzyloxy)-propionaldehyde **2b**. The possible syn and anti cycloadducts **3a**−**f** and **4a**−**f**, respectively, are also collected in Scheme 2.

In a previous work,[39] we have reported a computational study on the different conformations of (*S*)-2-methoxypropanal **2a** both in the gas phase and in solution. This aldehyde has also been studied by Frenking et al.[44] At the B3LYP/6-31G*, B3LYP(L1A1)/6-31G*, and MP2(SCIPCM)/6-31G*//HF(L1A1)/6-31G* levels, the relative

(29) MacroModel V5.0: Mohamadi, F.; Richards, N. G. J.; Guida, W. C.; Liskamp, R.; Lipton, M.; Caufield, C.; Chang, G.; Hendrickson, T.; Still, W. C. *J. Comput. Chem.* **1990**, *11*, 440.

(30) Parr, R. G.; Yang, W. *Density-Functional Theory of Atoms and Molecules*; Oxford: New York, 1989.

(31) (a) Becke, A. D. *J. Chem. Phys.* **1993**, *98*, 5648. (b) Becke, A. D. *Phys. Rev. A* **1988**, *38*, 3098. (c) Lee, C.; Yang, W.; Parr, R. G. *Phys. Rev. B* **1980**, 37, 785. (d) Vosko, S. H.; Wilk, L.; Nusair, M. *Can. J. Phys.* **1980**, *58*, 1200.

(32) See, for example: (a) Wiest, O.; Black, K. A.; Houk, K. N. *J. Am. Chem. Soc.* **1994**, *116*, 10336. (b) Wiest, O.; Houk, K. N.; Black, K. A.; Thomas, B., IV. *J. Am. Chem. Soc.* **1995**, *117*, 8594. (c) Goldstein, E.; Beno, B.; Houk, K. N. *J. Am. Chem. Soc.* **1996**, *118*, 6036. (d) Yoo, H. Y.; Houk, K. N. *J. Am. Chem. Soc.* **1997**, *119*, 2877.

(33) McIver, J. W.; Komornicki, A. K. *J. Am. Chem. Soc.* **1972**, *94*, 2625.

(34) Pople, J. A.; Schleyer, B.; Krishnan, R.; DeFrees, D. J.; Binkley, J. S.; Frisch, H.; Whiteside, R.; Hout, R. F., Jr.; Hehre, W. J. *Int. J. Quantum Chem. Symp.* **1981**, *15*, 269.

(35) (a) Binkley, J. S.; Pople, J. A. *Int. J. Quantum. Chem.* **1975**, *9*, 229. (b) Pople, J. A.; Binkley, J. S.; Seeger, R. *Int. J. Quantum Chem. Symp.* **1976**, *10*, 1.

(36) Reichardt, C. *Solvents and Solvent Effects in Organic Chemistry*; VCH: Weinheim, 1990; pp 147−170.

(37) (a) Tomasi, J.; Persico, M. *Chem. Rev.* **1994**, *94*, 2027. (b) Simkin, B. Ya.; Sheikhet, I. *Quantum Chemical and Statistical Theory of Solutions-A Computational Approach*; Ellis Horwood: London, 1995; pp 78−101. (c) Cramer, C. J.; Trhular, D., D. G. In *Reviews in Computational Chemistry*; Lipkowitz, K. B., Boyd, D. B., Eds.; VCH Publishers: New York, 1995; Vol. VI, pp 1−72.

(38) (a) Wong, M. W.; Wiberg, K. B.; Frisch, M. J. *J. Am. Chem. Soc.* **1992**, *114*, 523. (b) Wong, M. W.; Wiberg, K. B.; Frisch, M. J. *J. Am. Chem. Soc.* **1992**, *114*, 1645.

(39) Lecea, B.; Arrieta, A.; Cossío, F. P. *J. Org. Chem.* **1997**, *62*, 6485.

(40) (a) Wiberg, K. B.; Castejon, H.; Keith, T. A. *J. Comput. Chem.* **1996**, *17*, 185. (b) Wiberg, K. B.; Keith, T. A.; Frisch, M. J.; Murcko, M. *J. Phys. Chem.* **1995**, *99*, 9072. (c) Wiberg, K. B.; Rablen, P. R.; Rush, D. J.; Keith, T. A. *J. Am. Chem. Soc.* **1995**, *117*, 4261.

(41) Glendening, E. D.; Reed, A. E.; Carpenter, J. E.; Weinhold, F. NBO Version 3.1, Gaussian, Inc., 1995.

(42) Wiberg, K. B. *Tetrahedron* **1968**, *24*, 1083.

(43) Gong, L.; McAllister, M. A.; Tidwell, T. T. *J. Am. Chem. Soc.* **1991**, *113*, 6021.

(44) Frenking, G.; Köhler, K. F.; Reetz, M. T. *Tetrahedron* **1991**, *47*, 8991.

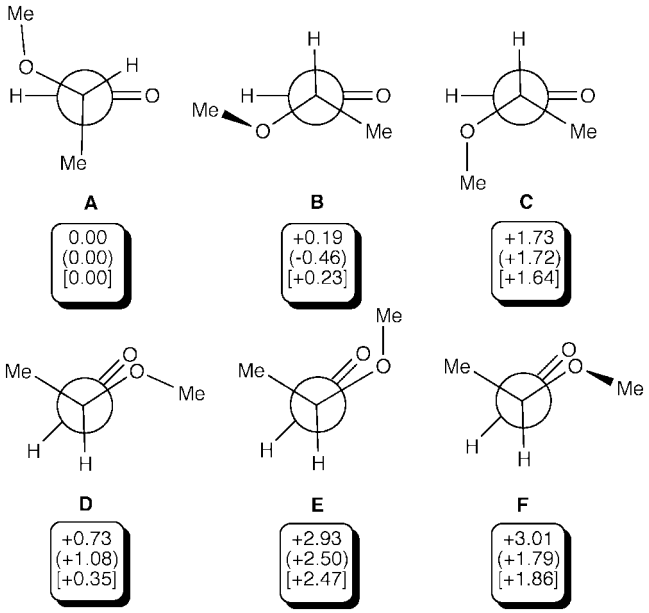

Figure 2. Six conformations of (*S*)-2-methoxypropanal at the B3LYP/6-31G* + ΔZPVE, B3LYP(L1A1)/6-31G* + ΔZPVE (in parentheses), and MP2(SCIPCM)/6-31G*//HF(L1A1)/6-31G* + ΔZPVE (in square brackets) levels. Numbers are relative energies in kcal/mol. The data in solution refer to $\epsilon = 9.08$ (dichloromethane).

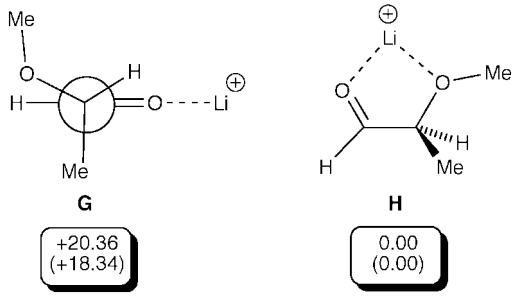

Figure 3. Two ion−molecule complexes resulting from the interaction between (*S*)-3-methoxypropanal and lithium cation. Numbers correspond to the relative energies (in kcal/mol) at the B3LYP/6-31G* + ΔZPVE and MP2/6-31G*//HF/6-31G* + ΔZPVE level (in parentheses).

energies of the different conformers are at those reported in Figure 2. According to these results, conformer **A** is the most stable one both in the gas phase and in dichloromethane solution, although the L1A1 model overestimates the stability of conformer **B**. Similarly, we have found[39] that when cations such as lithium are present, the chelated structure **H** is largely the most stable one, as shown in Figure 3.

We have studied first the possible reaction paths associated with the interaction between **2a** and dichloroketene **1a** to form either *syn*- or *anti*-**3a** (see Scheme 2). We have located two diastereomeric saddle points denoted as ***syn*-TSa** and ***anti*-TSa** in Figure 4. The corresponding activation and reaction energies, as well as the relative energies, are shown in Table 2. According to our results, ***syn*-TSa** is the lowest energy saddle point. Thus, at the MP2/6-31G*//HF/6-31G* and B3LYP/6-31G* levels, it is predicted that ***syn*-TSa** is 0.56 and 0.76 kcal/mol more stable than ***anti*-TSa**, respectively. The latter energy difference corresponds to a diastereomeric ratio

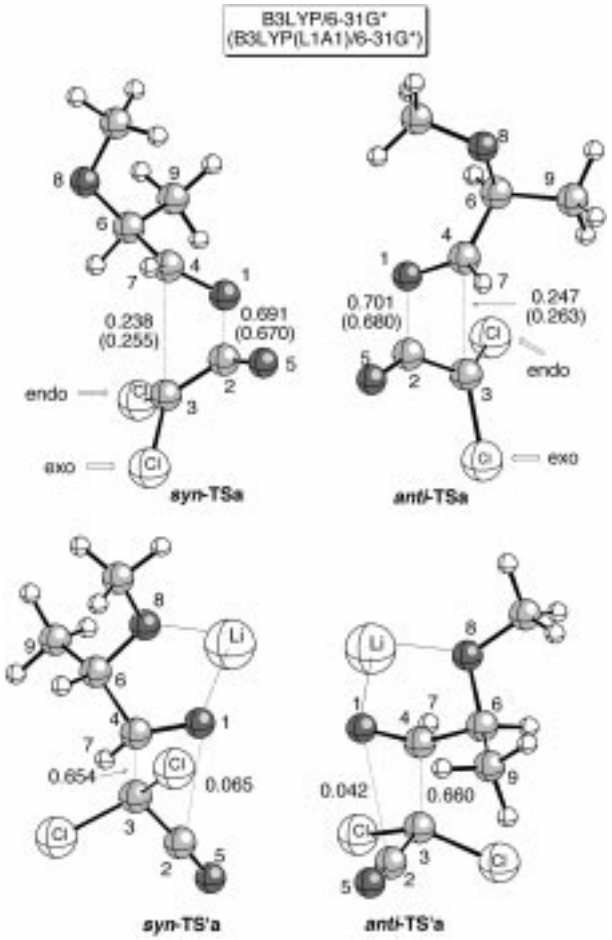

Figure 4. Ball and stick representations of diastereomeric saddle points **TSa** and **TS′a**. Numbers correspond to the Wiberg bond indices, computed at several theoretical levels. In this and Figures 5−8, unless otherwise stated, atoms are represented by increasing order of shadowing as follows: H, C, O.

of ca. 78:22 at 25 °C. Inclusion of solvent effects[45] results in lower computed activation energies and also in lower stereocontrol (see Table 2). For instance, the calculated activation energy at the B3LYP(SCIPCM)/6-31G*//B3LYP-(L1A1)/6-31G* is ca. 0.8 kcal/mol lower than that predicted in the gas phase. In addition, the $\Delta\Delta E_a$ value calculated at the same theoretical level is ca. 0.3 kcal/mol lower than that obtained in vacuo. This result is even more pronounced when electron correlation was approximately evaluated using the MP2 approach. Thus,

(45) One reviewer has suggested that hydrogen bonding between Et_3N^+H (formed in the course of the generation of the ketene, vide infra) and the sp^3-hybridized oxygen atom of the aldehyde could be more important than solvent effects. To check this hypothesis, we have optimized the complex between ammonium cation and hydroxyacetaldehyde. We have found that at the HF/6-31G* level the cation forms a hydrogen bond with the hydroxylic oxygen. However, at the B3LYP/6-31G* level, hydrogen bonding occurs through the oxygen of the carbonyl group. These interactions should be lower at the TS and with bulkier substituents. The electrostatic effect, if any, should be not very directional in character and will not affect significantly the stereochemical outcome.

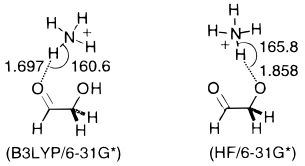

Table 1. Activation Energies[a,b] (ΔE_a, kcal/mol), and Reaction Energies[a,b] (ΔE_{rxn}, kcal/mol), Associated with the [2 + 2] Cycloaddition Reaction between Ketenes 1a−c and Aldehyde 2a (Conformers A and H) To Yield 2-Oxetanones *syn*- and *anti*-3a,c,e

	syn products			anti products					
level	ΔE_a	$\Delta E'_a$	ΔE_{rxn}	ΔE_a	$\Delta\Delta E_a$	$\Delta E'_a$	$\Delta\Delta E'_a$	ΔE_{rxn}	$\Delta\Delta E_{rxn}$
			1a + 2a → 3a						
MP2/6-31G*//HF/6-31G*	23.02	8.34	−42.19	23.58	+0.56	14.37	+6.03	−43.00	−0.81
B3LYP/6-31G*	19.62	16.38	−32.05	20.38	+0.76	21.77	+5.39	−32.50	−0.45
MP2(L1A1)/6-31G*//HF(L1A1)/6-31G*	22.56		−42.12	22.67	+0.11			−44.02	−1.90
B3LYP(L1A1)/6-31G*	18.68		−31.82	19.20	+0.52			−33.30	−1.48
HF(SCIPCM)/6-31G*//HF(L1A1)/6-31G*	37.03		−28.48	37.14	+0.11			−29.74	−1.26
MP2(SCIPCM)/6-31G*//HF(L1A1)/6-31G*	23.34		−41.80	23.42	+0.08			−42.76	−0.96
B3LYP(SCIPCM)/6-31G*//B3LYP(L1A1)/6-31G*	18.82		−31.30	19.25	+0.43			−31.99	−0.69
			1b + 2a → 3c						
MP2/6-31G*//HF/6-31G*	26.91	7.38	−30.35	30.23	+3.32	8.58	+1.20	−30.87	−0.52
B3LYP/6-31G*	26.96	11.14	−24.11	29.22	+2.26	11.26	+0.12	−24.45	−0.34
			1c + 2a → 3e						
MP2/6-31G*//HF/6-31G*	27.49	−0.36	−34.33	30.52	+3.03	2.62	+2.98	−39.36	−5.03
B3LYP/6-31G*	28.23	8.31	−24.37	29.94	+1.71	9.39	+1.08	−25.70	−1.33

[a] ZPVE corrections, computed at the optimization level. [b] $\Delta\Delta E_a$ and $\Delta\Delta E_{rxn}$ are the relative energies with respect to the syn cycloadduct.

Table 2. Main Second-Order Energies ($\Delta E^{(2)}$), kcal/mol) in the Transition Structures TSa,c,e and TS′a,c,e

level	$\phi_{XC} \rightarrow \phi^*_{\neq}$	$\phi_{\neq} \rightarrow \phi^*_{XC}$	$\phi_{XC} \rightarrow \phi^*_{\neq}$	$\phi_{\neq} \rightarrow \phi^*_{XC}$
	***syn*-TSa**		***anti*-TSa**	
B3LYP/6-31G*	3.71[a]	1.47[b]	12.46[c]	0.00
B3LYP(L1A1)/6-31G*	2.87[a]	2.05[b]	12.69[c]	0.00
	***syn*-TS′a**		***anti*-TS′a**	
B3LYP/6-31G*	2.18[f]	1.22[g]	3.14[d]	1.60[e]
	***syn*-TSc**		***anti*-TSc**	
B3LYP/6-31G*	4.42[a]	1.87[b]	1.82[d]	3.39[e]
	***syn*-TS′c**		***anti*-TS′c**	
B3LYP/6-31G*	1.64[d]	2.34[e]	2.42[d]	3.00[e]
	***syn*-TSe**		***anti*-TSe**	
B3LYP/6-31G*	4.42[a]	1.94[b]	8.42[c]	1.04[b]
	***syn*-TS′e**		***anti*-TS′e**	
B3LYP/6-31G*	1.78[f]	1.14[g]	2.82[d]	2.30[e]

[a] $\Delta E^{(2)}[\sigma_{6,8} \rightarrow \pi^*_{1,4}]$. [b] $\Delta E^{(2)}[\pi_{1,4} \rightarrow \sigma^*_{6,8}]$. [c] $\Delta E^{(2)}[\sigma_{6,7} \rightarrow \pi^*_{1,4}]$. [d] $\Delta E^{(2)}[\sigma_{6,8} \rightarrow \sigma^*_{3,4}]$. [e] $\Delta E^{(2)}[\sigma_{3,4} \rightarrow \sigma^*_{6,8}.]$ [f] $\Delta E^{(2)}[\sigma_{6,9} \rightarrow \sigma^*_{3,4}]$. [g] $\Delta E^{(2)}[\sigma_{3,4} \rightarrow \sigma^*_{6,9}.]$

at the MP2(SCIPCM)/6-31G*//HF(L1A1)/6-31G* level, virtually no stereoselection is predicted ($\Delta\Delta E_a$ = 0.08 kcal/mol), a result that is not in agreement with the experimental evidence (vide infra). On the basis of this result, we conclude that the B3LYP method is more appropriate for the evaluation of stereocontrol in this kind of reactions. The major isomer predicted for this cycloaddition is *syn*-**3a**, which corresponds to a non-Felkin diastereoselectivity. Interestingly, when 2-oxetanones are synthesized using the enolate methodology developed by Danheiser,[46] *anti*-2-oxetanones are preferably formed with excellent stereocontrol, as we have shown previously.[47]

Our calculations also predict that anti cycloadducts are more stable than their syn isomers, as shown in Table 1. It is noteworthy that the minimum energy conformers in both diastereomers are quite different (see Figure 5). In the anticycloadducts, the two C−O bonds are in an antiperiplanar relationship and the ϕ = O8−C6−C4−O1 dihedral angles lie in the range 174.7−179.3°. In contrast, the *syn*-2-oxetanones show minimum energy conformations in which the same dihedral angle varies from 62.3° to 69.7°, thus indicating that both groups are gauche to each other. In summary, both thermodynamic control and enolate methodology yield the opposite stereochemical outcome with respect to the [2 + 2] cycloaddition under kinetic control.

Given the high electrophilicity of ketene **1a**, the ipso interaction is the predominant one in these transition structures (see Table 1 of the Supporting Information for geometrical details). Thus, in both isomers of **TSa** the bond indices between the O1 and C2 atoms are ca. 0.70, whereas those associated with the formation of the C3−C4 bond are ca. 0.25 (see Figure 4, structures ***syn*-** and ***anti*-TSa**). The main difference between ***syn*-** and ***anti*-TSa** is that in the former the C6−O8 bond is almost antiperiplanar to the C3−C4 bond being formed, the dihedral angle ϕ = C3−C4−C6−O8 being in the range 170.7−178.5° (see Table 1 of the Supporting Information). In ***anti*-TSa**, the C6−H7 bond is almost eclipsed to the C3−C4 bond, the dihedral angle ξ = C3−C4−C6−H7 varying from 1.0 to 10.3°. On the other hand, if we define the nucleophilic angle of attack in the form α_N = C3−C4−O1, we observe that in both TSs this value is always lower than 90°. Therefore, the values of α_N do not correspond to the Bürgi−Dunitz trajectories[48] usually observed in 1,2-nucleophilic additions to carbonyl compounds. If chelation effects are not involved, these latter processes are usually associated with Felkin−Ahn diastereoselectivities.[49]

The origins of the stereochemical outcome in this reaction can be rationalized as the summation of steric, electrostatic, and stereoelectronic effects. The latter ones can in turn be understood by examining the substituent effects on the MOs of the parent system. Figure 6 shows the canonical FMOs of the transition structure associated with the simplest case, namely [2 + 2] cycloaddition

(46) (a) Danheiser, R. L.; Nowick, J. S. *J. Org. Chem.* **1991**, *56*, 1176. (b) Danheiser, R. L.; Choi, Y. M.; Menichincheri, M.; Stoner, E. J. *J. Org. Chem.* **1993**, *58*, 322.

(47) Arrastia, I.; Lecea, B.; Cossío, F. P. *Tetrahedron Lett.* **1996**, *37*, 245.

(48) (a) Bürgi, H. B.; Dunitz, J. D.; Scheffer, E. *J. Am. Chem. Soc.* **1973**, *95*, 5065. (b) Bürgi, H. B.; Dünitz, J. D.; Lehn, J. M. *Tetrahedron* **1974**, *30*, 1563.

(49) Gawley, R. E.; Aubé, J. *Principles of Asymmetric Synthesis*; Pergamon: Oxford, 1996; pp 121−160 and references therein.

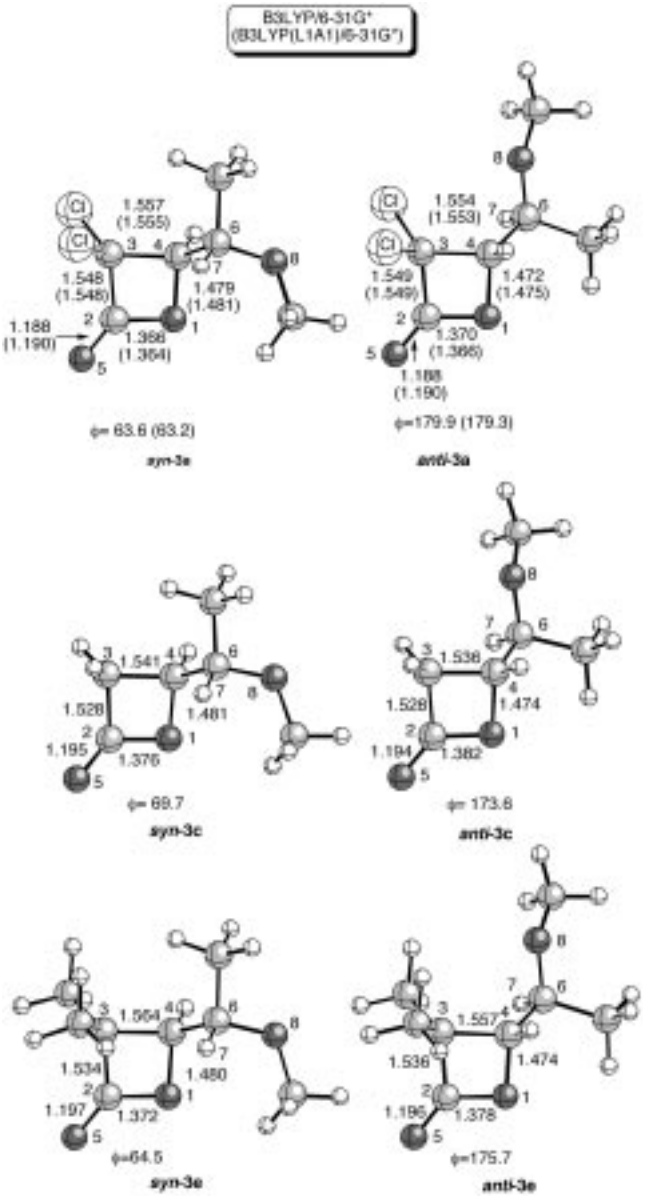

Figure 5. Ball and stick representations of the lowest energy conformations of *syn*- and *anti*-2-oxetanones **3a**,**c**,**e**. Bond distances and angles are given in Å and deg, respectively. ϕ is the O8−C6−C4−O1 dihedral angle and is reported as an absolute value.

between ketene and formaldehyde.[50] As it can be seen, both FMOs result mainly from the two possible combinations between the LUMO of formaldehyde (basically a π^*_{CO} orbital) and the distorted HOMO of ketene (the $2b_1$ MO within the C_{2v} symmetry). The HOMO of the parent TS is dominated by the distorted σ interaction between C3 and C4. This MO has an energy of −6.83 eV, and

(50) This TS has been calculated previously at other theoretical levels (see refs 16−18). Its main geometrical features at the B3LYP/6-31G* level are the following (bond distances are given in Å and numbers in parentheses correspond to the bond indices):

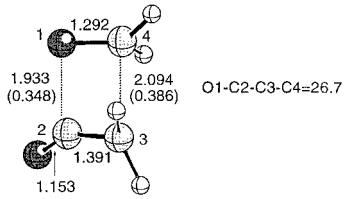

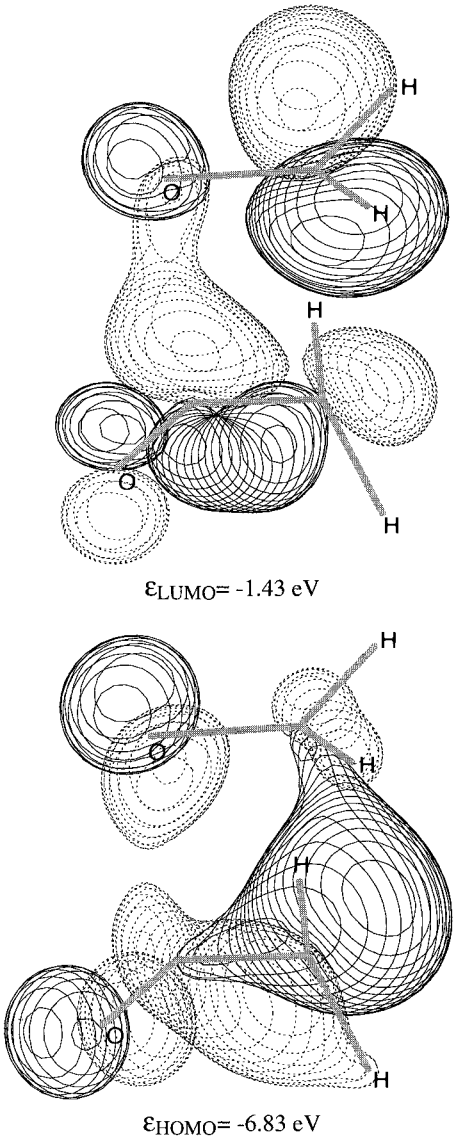

Figure 6. Computer plot of the FMO's of the transition structure corresponding to the [2 + 2] cycloaddition between ketene and formaldehyde, calculated at the B3LYP/6-31G*. Contour plot has been fixed at 0.065 e/bohr^3.

therefore, the C3···C4 bond can act as a very efficient donor. Similarly, the energy of the LUMO of this TS is −1.43 eV at the B3LYP/6-31G* level, and therefore, the C3 atom constitutes a strong acceptor. Consequently, the C3 atom will be very sensitive to the effect of donating substituent of the aldehyde moiety and the C3−C4 bond being formed will interact efficiently with σ-acceptors at C3.

To quantify the above-mentioned stereoelectronic effects involved in ***syn-*** and ***anti-*****TSa**, we have analyzed the most relevant two-electron interactions between the corresponding NBOs. In some cases, the NPA assigns the acceptor character of C3 to the $\pi^*_{3,4}$ localized orbital. This is consistent with the high participation of this orbital in the FMOs represented in Figure 6. We have separated in two groups the stereoelectronic effects between the chiral group X_C, namely the (*S*)-1-methoxyethyl group, and the ring being formed. In the first one, we have included the $\phi_{X_C} \rightarrow \phi^*_{\ddagger}$ interactions between filled NBOs of X_C and vacant NBOs localized on the ring being formed. In the second group, we have collected the

Scheme 3

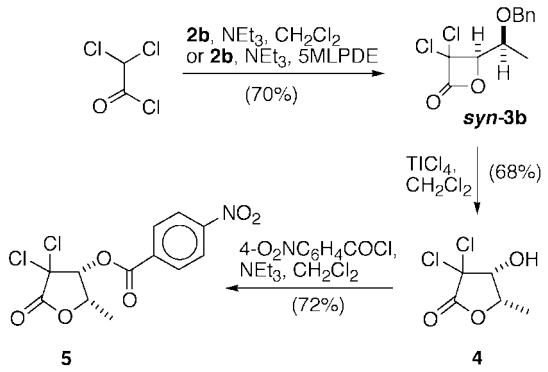

most significant interactions of type $\phi_{\ddagger} \rightarrow \phi^*_{X_C}$, namely between a filled NBO of the ring being formed and an antibonding NBO associated with the chiral group. The result of this analysis is reported in Table 2. From the data included in Table 2, it is clear that in both ***syn-*** and ***anti*-TSa** the former type of interaction is the predominant one. Thus, in ***syn*-TSa** the main term is the $\sigma_{6,8} \rightarrow \pi^*_{1,4}$ contribution, whereas in ***anti*-TSa** the most important term corresponds to the $\sigma_{6,7} \rightarrow \pi^*_{1,4}$ interaction. Given that the C−H bond is a better donor than the C−O bond,[39] the $\Delta E^{(2)}$ terms associated with the $\sigma_{6,7} \rightarrow \pi^*_{1,4}$ interaction are much more important than those corresponding to the $\sigma_{6,8} \rightarrow \pi^*_{1,4}$ donation (see Figure 4). However, ***syn*-TSa** is calculated to be of lower energy than ***anti*-TSa** (vide supra). It can be therefore concluded that two-electron stereoelectronic effects do not determine the stereocontrol of the reaction. Given that in these transition structures the $[{}_{\pi}2_s + ({}_{\pi}2_s + {}_{\pi}2_s)]$ geometry imposes a significant torsion around the C2−C3 bond, in ***anti*-TSa** there is a steric repulsive interaction between the methyl group and the endo chlorine atom, whereas in ***syn*-TSa** the methyl group is at the opposite side of the endo chlorine atom (see Figure 4). In addition, there is a repulsive Coulombic interaction between the exo chlorine and the O8 atom in ***anti*-TSa**. The superposition of all these effects results in the preferential formation of ***syn*-3a** under kinetic control.

To verify the validity of this prediction, we carried out the reaction between **1a**, generated in situ by treatment of dichloroacetyl chloride with triethylamine, and (*S*)-2-(benzyloxy)propionaldehyde **2b**. After 30 min of reaction at 0−5 °C, cycloadduct **3b** was isolated in 70% yield as a single stereoisomer after purification by flash chromatography (see Scheme 3). Inspection of the crude reaction mixture by ^{1}H NMR revealed that only one isomer was formed in the course of the [2 + 2] cycloaddition. To verify the stereochemistry of the cycloadduct, the benzyl group was removed by treatment with $TiCl_4$, followed by transesterification to form the γ-lactone **4**,[47] which was further transformed into its solid 4-nitrobenzoyl ester derivative **5**. Both butyrolactones **4** and **5** exhibited low coupling constants between the protons at C4 and C5 (3.2 and 3.4 Hz, respectively, see Experimental section), together with a low nuclear Overhauser effect (NOE) over the proton at C4 when the methyl group was presaturated. These spectral data were assigned to a cis configuration for these products[51] and, therefore, to a syn configuration for the starting propiolactone **3b**.

(51) Jaime, C.; Segura, C.; Dinarés, I.; Font, J. *J. Org. Chem.* **1993**, *58*, 154.

In a preliminary communication,[21] we have reported that the [2 + 2] cycloaddition between ketenes and aldehydes can be efficiently promoted using 5 M solutions of lithium perchlorate in diethyl ether (5 M LPDE). This polar solvent has proved to be useful in [4 + 2] cycloaddition reactions and other processes.[52] Therefore, we performed the reaction between dichloroacetyl chloride and **2b** in 5 M LPDE and in the presence of 1.1 equiv of triethylamine. Under these conditions, cycloadduct ***syn*-3b** was obtained as a single stereoisomer in 70% yield after 30 min of reaction at 0−5 °C. This cycloadduct exhibited identical spectroscopic properties with respect to those previously found for ***syn*-3b**. Therefore, the sense of stereocontrol in dichloromethane and in 5 M LPDE was found to be the same.

The origins of the efficiency of 5 M LPDE in promoting thermally allowed cycloadditions have been the subject of a vivid debate. Thus, several authors[52] have attributed this effect to the high internal pressure generated by the solvent as well as to other nonspecific solvent effects. Others investigators,[53] however, explain the observed acceleration in terms of Lewis acid catalysis by the lithium cation. In this respect, we have recently reported[54] that in several Diels−Alder reactions between nitroalkenes and dienes 5 M LPDE (and 4 M lithium perchlorate in nitromethane as well) promotes formation of the cycloadducts that are obtained under purely thermal conditions. This result is significant, since it has been reported that nitroalkenes can act as dienes if Lewis acids are present, to yield cyclic nitronates, which in turn can suffer a variety of interesting transformations.[55]

Despite these precedents, Lewis acid complexation of the lithium cation cannot be in principle ruled out in the [2 + 2] cycloaddition between carbonyl compounds and ketenes. Although complexation of a solvated lithium cation to a carbonyl compound is not a favored process in an ethereal solvent,[56] the resulting chelated structure can be more reactive than the uncomplexed carbonyl compound. Therefore, we decided to explore computationally the reaction between **2a** complexed with a lithium cation[57] and dichloroketene **1a**. The two transition structures ***syn*-TS′a** and ***anti*-TS′a** are shown in Figure 4, and their geometrical and energetic features are reported in Table 1 and in Table 1 of the Supporting Information. As can be observed, in both saddle points the lithium atom is coordinated to the O1 and O8 atoms, similar to the chelated structure **H** depicted in Figure 3. Nonchelated structures spontaneously converged to the chelated ones upon optimization.

Our results indicate that in the case of the syn diastereomer lithium chelation induces a lowering in the activation energy of 3.24 kcal/mol at the B3LYP/6-31G* + ΔZPVE level. At the MP2/6-31G*//HF/6-31G* + ΔZPVE level, we have obtained a lowering of 14.68 kcal/mol, which is probably too large.[16] In any case, the former value is in qualitative agreement with the acceleration experimentally observed by us. In addition, the energy difference between both transition structures

(52) (a) Grieco, P. A.; Nunes, J. J.; Gaul, M. D. *J. Am. Chem. Soc.* **1990**, *112*, 4595. (b) Waldmann, H. *Angew. Chem., Int. Ed. Engl.* **1991**, *30*, 1306. (c) Grieco, P. A.; Handy, S. T.; Beck, J. P. *Tetrahedron Lett.* **1994**, *35*, 2663. (d) Grieco, P. A. *Aldrichim. Acta* **1991**, *24*, 59.

(53) Forman, M. A.; Dailey, W. P. *J. Am. Chem. Soc.* **1991**, *113*, 2761.

(54) Ayerbe, M.; Cossío, F. P. *Tetrahedron Lett.* **1995**, *36*, 4447.

(55) Denmark, S. E.; Thorarensen, A. *Chem. Rev.* **1996**, *96*, 137.

(56) Chen, X.; Hortelano, E. R.; Eliel, E. L.; Frye, S. V. *J. Am. Chem. Soc.* **1992**, *114*, 1778.

is calculated to be 6.03 and 5.39 kcal/mol in favor of the syn cycloadduct at the MP2/6-31G*//HF/6-31G* + ΔZPVE and B3LYP/6-31G* + ΔZPVE levels, respectively (see the $\Delta\Delta E'_a$ values in Table 1). Therefore, these calculations predict the same sense of stereoselection observed for the **1a** + **2a** → **3a** process.

Both ***syn-*** and ***anti*-TS′a** diastereomeric structures show important differences with respect to their nonlithiated analogues (see Figure 4 and Table 1 of the Supporting Information). Thus, the C3···C4 bond is now largely more developed than the O1···C2 bond. For example, in ***syn*-TS′a**, the respective bond distances are calculated to be 1.774 and 2.573 Å at the B3LYP/6-31G* level, which correspond to Wiberg NBA bond indices of 0.654 and 0.065, respectively. Therefore, the reaction can be described as a two-stage process, in which the main interaction in the transition structure corresponds to a nucleophilic attack of the ketene over the chelated (and more electrophilic) aldehyde. The α_N value is found to be 105.3° at the B3LYP/6-31G* level, which is now in line with the Bürgi−Dunitz trajectory. In summary, the stereochemistry of the lithium-assisted version of the reaction is what one would expect from the cyclic Cram model. Thus, in ***syn*-TS′a**, the attack of the ketene takes place through the less hindered side of the chelated aldehyde, whereas in ***anti*-TS′a** the attack occurs through the side of the methyl group, thus resulting in a destabilizing steric interaction between the methyl group and a chlorine atom, as well as a distortion in the cyclic structure of the chelated aldehyde (see Figure 4). Therefore, in this case, a more reactive species (**H** in Figure 3) is actually more selective (compare the $\Delta\Delta E_a$ and $\Delta\Delta E'_a$ values in Table 1), as is predicted in the cyclic Cram model.[56,58] It is important to note that in these calculations with saddle points ***syn-*** and ***anti*-TS′a** solvation of the lithium cation by the ethereal solvent has not been considered. However, it is expected that the effect of this simplification is similar for both diastereomeric structures and therefore will not affect significantly their relative energies. In summary, we can conclude that if lithium perchlorate accelerates the cycloaddition rate via ion−molecule complexation the sense of stereoselection is the same that observed for the purely thermal cycloaddition. Therefore, *both* reaction paths are in agreement with our experimental findings.

The next step of our study was to explore computationally the behavior of ketene **1b** itself toward aldehyde **2a** to yield 2-oxetanones ***syn-*** and ***anti*-3c**. The chief geometric features of the transition structures ***syn-*** and ***anti*-TSc** are reported in Table 1 of the Supporting Information and in Figure 7. Given the lower electrophilicity of ketene with respect to dichloroketene, the O1−C2 and C3−C4 bond distances in these TSs are larger and shorter than in the preceding case, respectively. The B3LYP/6-31G* method predicts a higher degree of advancement in the former interaction, particularly in the case of ***syn*-TSc**.

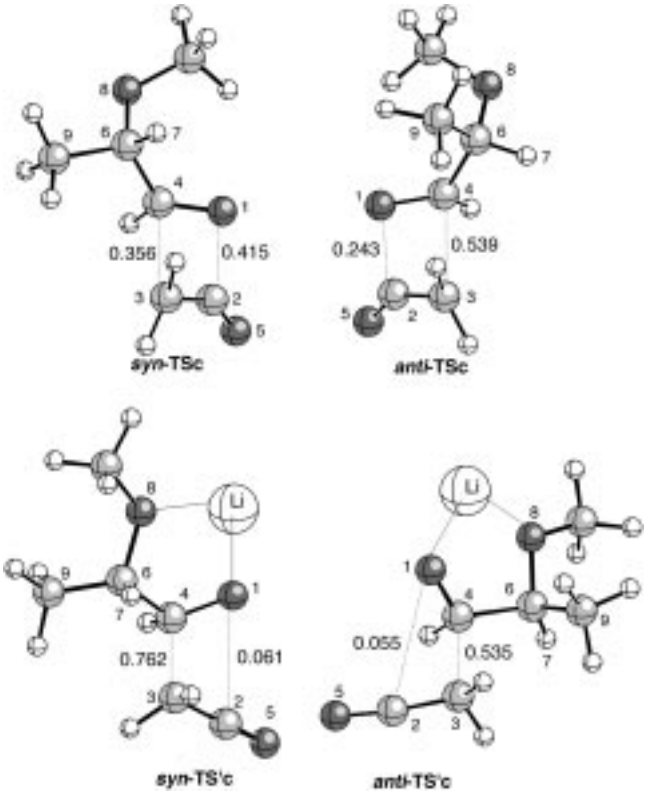

Figure 7. Ball and stick representations of diastereomeric saddle points **TSc** and **TS′c**. Numbers correspond to the Wiberg bond indices.

Since the interaction of the *endo*-hydrogen atoms of ketene and the substituent of the aldehyde is lower than in the preceding case, there is a remarkable freedom for the chiral group of **2a** to adopt the optimal conformation. Thus, in ***syn*-TSc** the value of ϕ is almost 180°, thus indicating that the C6−O8 and C3···C4 bonds are perfectly antiperiplanar to each other (see Table 1 of the Supporting Information). Inclusion of electron correlation in this saddle point induces an enlargement of the C3···C4 bond distance, the energy associated to the $\pi_{1,4} \rightarrow \sigma^*_{6,8}$ interaction being only 1.87 kcal/mol at the B3LYP/6-31G* level (see Table 2). The highest stabilizing donation for this saddle point is 4.42 kcal/mol, a value that is associated with the reverse $\sigma_{6,8} \rightarrow \pi^*_{1,4}$ donation. In the case of ***anti*-TSc**, the main two electron interaction is the $\sigma_{3,4} \rightarrow \sigma^*_{6,8}$ donation, with a second-order energy value of 3.39 kcal/mol at the B3LYP/6-31G* level. Since in ***anti*-TSc** the C3···C4 bond distance is shorter than in ***syn*-TSc**, the C3···C4 and C6−C8 bonds cannot adopt an antiperiplanar conformation, and therefore, the magnitude of the $\sigma_{3,4} \rightarrow \sigma^*_{6,8}$ interaction, although significant, is not optimal.

The global result of all these combined interactions is that ***anti*-TSc** is calculated to be 3.32 and 2.26 kcal/mol

(57) One reviewer has suggested that lithium complexation could also take place through the oxygen atom of the ketene. Attempts to locate saddle points in which the lithium was complexed to O5 invariably converged to the reported TSs upon optimization. On the other hand, the ΔE value of the following isodesmic equation

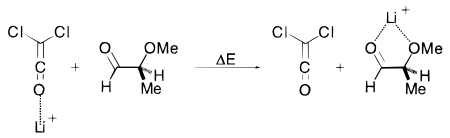

was found to be −38.2 kcal/mol at the B3LYP/6-31G* + ΔZPVE level, thus suggesting preferential aldehyde complexation also in the substrates. This is in agreement with the well-known participation of the resonance form **II** in ketenes (see ref 2, p 33):

(58) Cram, D. J.; Kopecky, K. R. *J. Am. Chem. Soc.* **1959**, *81*, 2748.

Scheme 4

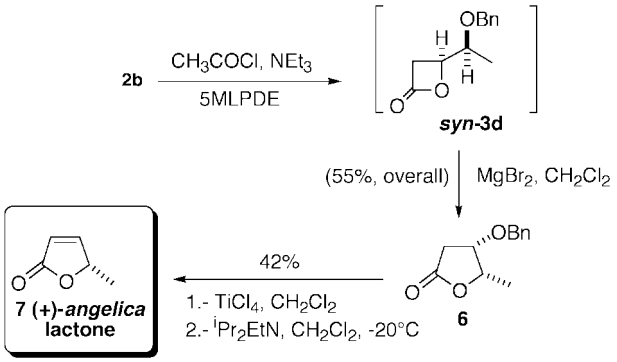

less stable than ***syn*-TSc** at MP2/6-31G*//HF/6-31G* + ΔZPVE and B3LYP/6-31G* + ΔZPVE levels, respectively. It is also noteworthy that the calculated activation energies are higher than in the preceding case. Thus, the ΔE_a value for the **1b** + **2a** → ***syn*-3c** process is calculated to be 7.34 kcal/mol larger than that found for the **1a** + **2a** → ***syn*-3a** process at the B3LYP/6-31G* + ΔZPVE level (see Table 1). Therefore, the **1b** + **2a** → **3c** transformation is predicted to be significantly more difficult than the former one, although the computed ΔE_a values are probably too low at these theoretical levels[59] (vide infra).

We have also calculated the lithium-assisted version of the reaction between ketene and (*S*)-2-methoxypropanal. We have located two diastereomeric saddle points ***syn*-TS′c** and ***anti*-TS′c** associated with the reaction coordinate. Their chief geometrical features are quite similar to those found for the diastereomeric **TS′a** saddle points. The C3···C4 bond is again substantially more developed than the O1···O2 bond (see the corresponding bond orders in Figure 7). The α_N values of ***syn*-** and ***anti*-TS′c** are of ca. 107°, and once again, their shape is concordant with the cyclic (chelated) Cram model. At the MP2/6-31G*//HF/6-31G* + ΔZPVE level, it is predicted that ***syn*-TS′c** is 1.20 kcal/mol lower in energy than ***anti*-TS′c**. This should correspond to a ca. 89:11 ratio between ***syn*-** and ***anti*-3c**. At the B3LYP/6-31G* level, the difference between ***syn*-** and ***anti*-TS′c** is lower (see Table 1). We have found that inclusion of solvent effects does not modify the sense of stereoselection. Following a suggestion made by one reviewer, we have included two water molecules around the lithium cation to model the ethereal solvent, and we have computed the relative energies. At the B3LYP(SCIPCM)/6-31G*//HF/6-31G* + ΔZPVE level, we have found that ***syn*-TS′c·2H$_2$O** is 1.06 kcal/mol more stable than ***anti*-TS′c·2H$_2$O** (see Figure 1 and Table 2 of the Supporting Information).

We have studied experimentally the cycloaddition between ketene **1b**, generated in situ from acetyl chloride and aldehyde **2b** (Scheme 4). After 12 h of reaction at room temperature, no cycloaddition products were detected from inspection of the reaction mixture. This result seems to support that the ΔE_a values computed for this reaction are systematically too low. In contrast, when the reaction was performed in 5 M LPDE, formation of 2-oxetanone **3d** was observed after 4 h of reaction at room temperature. Compound **3d** was unequivocally characterized by a characteristic carbonyl resonance in its IR spectrum at 1823 cm^{-1} and by the 300 MHz ^{1}H NMR spectrum of the crude reaction mixture (see Figure 2 of the Supporting Information). Treatment of ***syn*-3d** with magnesium dibromide gave butyrolactone **6** in a 55% overall yield from **2b**. Compound **6** was treated with $TiCl_4$ and then with diisopropylethylamine at −20 °C for 5 h to give (+)-angelica lactone **7** in 42% yield. The structure of this naturally occurring compound was verified from the reported physical and spectroscopic data.[60] Therefore, the reaction between aldehyde **2b** and ketene **1b** was proved to be feasible, provided that the reaction was carried out using 5 M LPDE as solvent. Under these conditions, a single diastereomer was detected, and its structure was assigned to ***syn*-3d** on the basis of the stereochemistry of compound **6** and is again in agreement with the computational results. On the other hand, our method provides a straightforward synthesis of (+)-angelica lactone **7** with total stereocontrol. It is noteworthy that in this case the enolate approach does not yield satisfactory results. For instance, reaction between **2b** and lithium enolate derived from *tert*-butyl acetate yields the two possible syn and anti *β*-hydroxy esters with virtually no stereoselection.[61]

We have also studied computationally the interaction between dimethylketene **1c** and (*S*)-2-methoxypropanal **2a**. The two diastereomeric transition structures, ***syn*-** and ***anti*-TSe**, are depicted in Figure 8. The shape of these saddle points closely resembles those already described for the **1b** + **2a** → **3c** process. The characteristic angles α_N, ξ, and ϕ are also similar for the two diastereomeric saddle points. In this case, the low electrophilicity of the ketene results in an enlargement of the activation energy. Thus, the activation energy computed for the **1c** + **2a** → ***syn*-3e** process is found to be of 4.47 and 8.61 kcal/mol higher than that computed for the **1a** + **2a** → ***syn*-3a** process at the MP2/6-31G*//HF/6-31G* + ΔZPVE and B3LYP/6-31G* + ΔZPVE levels, respectively. This means that the reactions using dimethylketene should be even more difficult than those using ketene. On the other hand, the interaction between the endo methyl group and the (*S*)-1-methoxyethyl group is larger than in the preceding case, and therefore, the difference in energy between the two diastereomeric saddle points is larger than between ***syn*-** and ***anti*-TSc**. Thus, ***syn*-TSe** is predicted to be 3.03 and 1.71 kcal/mol more stable than ***anti*-TSe** at the MP2/6-31G*//HF/6-31G* + ΔZPVE and B3LYP/6-31G* + ΔZPVE levels, respectively. In the case of the lithium-assisted saddle points, the $\Delta\Delta E'_a$ values are 2.98 and 1.08 kcal/mol, respectively, both of them in favor of the formation of ***syn*-3e**.

The verification of these predictions is shown in Scheme 5. Reaction of 2-methylpropionyl chloride with **2b** in the presence of triethylamine and 5 M LPDE gave cycloadduct ***syn*-3f** as the only stereoisomer detectable by NMR analysis on the crude reaction mixture. Depro-

(59) As we have previously reported, in this reaction the magnitudes of the activation energies are underestimated at the MP2/6-31G* level (see ref 16). Probably, this deficiency can be extended to the B3LYP/6-31G* level. For recent studies on this problem, see: (a) Fabian, W. M. F.; Kollenz, G. *J. Org. Chem.* **1997**, *62*, 8497. (b) Durant, J. L. *Chem. Phys. Lett.* **1996**, *256*, 595. (c) Glukhovtsev, M. N.; Bach, R. D.; Pross, A.; Radom, L. *Chem. Phys. Lett.* **1996**, *260*, 558.

(60) (a) Ortuño, R. M.; Alonso, D.; Cardellach, J.; Font, J. *Tetrahedron* **1987**, *43*, 2191. For the synthesis of the (−)-(*R*)-*angelica* lactone from D-ribonolactone, see: (b) Camps, P.; Cardellach, J.; Corbera, J.; Font, J.; Ortuño, R. M.; Ponsatí, O. *Tetrahedron* **1983**, *39*, 395. (c) Chen, S.-Y.; Joullié, M. *J. Org. Chem.* **1984**, *49*, 2168.

(61) Reetz, M. T. *Angew. Chem., Int. Ed. Engl.* **1984**, *23*, 1984 and references therein. See also: Braun, M. *Angew. Chem., Int. Ed. Engl.* **1987**, *26*, 24.

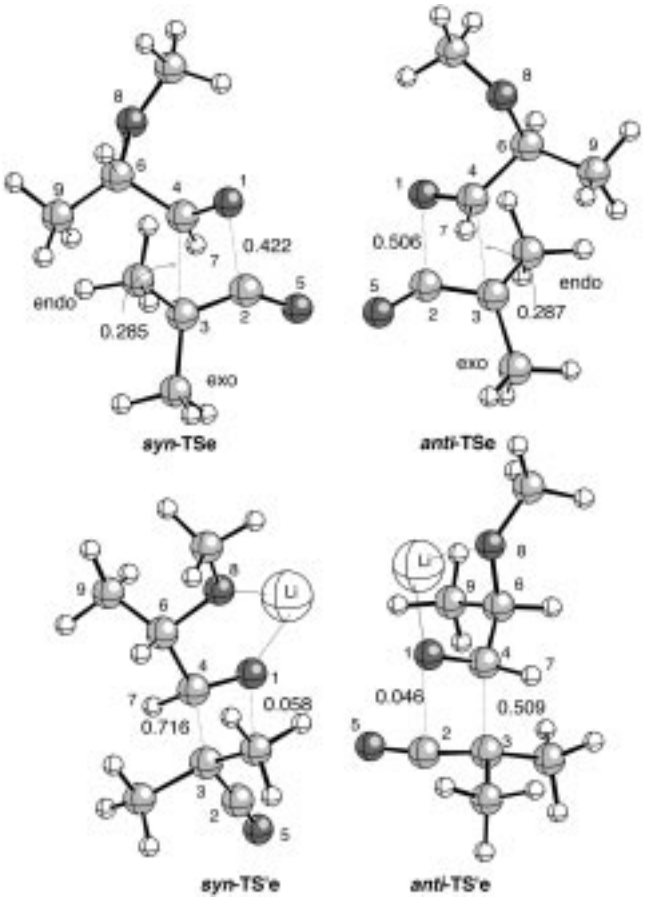

Figure 8. Ball and stick representations of diastereomeric saddle points **TSe** and **TS′e**. Numbers correspond to the Wiberg bond indices.

Scheme 5

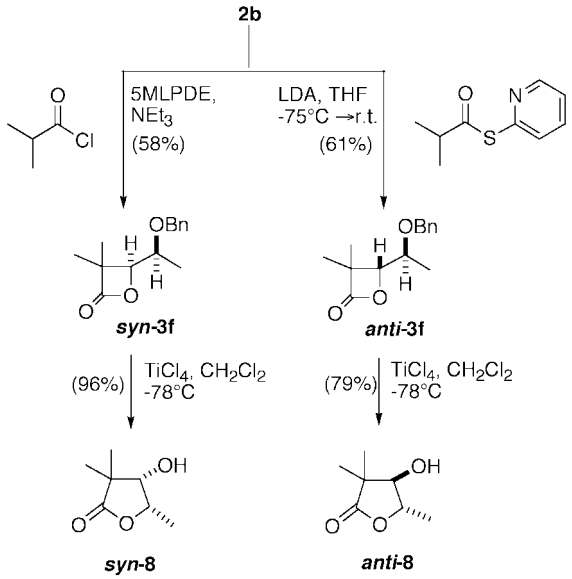

tection of the benzyloxy group followed by in situ transesterification gave the butyrolactone ***syn*-8** in excellent yield. The *syn*-stereochemistry of this compound was unequivocally established on the basis of the coupling constant between the C4-H and the C5-H methinic protons. The experimental value of this coupling constant is 3.7 Hz, a value in excellent agreement with that predicted by Jaime *et al.*[51] ($J_{4,5}$ = 3.8 Hz). On the other hand, reaction between 2-pyridyl isobutanethioate and **2b** in the presence of LDA under the conditions reported by Danheiser gave 2-oxetanone ***anti*-3f** in 61% yield. When the same reaction was performed using **2b** and phenyl isobutanethioate, the yield of ***anti*-3f** was only 39%. This compound, when subjected to the deprotection−transesterification sequence (see Scheme 5), yielded γ-lactone ***anti*-8** in 79% yield after purification by flash chromatography. The coupling constant between the C4-H and C5-H methinic protons was found to be 7.9 Hz, a value again in excellent agreement with that obtained by Jaime[51] ($J_{4,5}$ = 7.4 Hz). Therefore, the enolate and [2 + 2] approaches yield opposite stereochemistries, with complete stereocontrol in both cases, thus showing the complementary character of both methodologies.

Conclusions

From the combined computational and experimental results reported in this study the following conclusions can be drawn:

(i) The [2 + 2] cycloaddition between C_{2v} symmetric ketenes and homochiral aldehydes takes place through a concerted [$_\pi 2_s$ + ($_\pi 2_s$ + $_\pi 2_s$)] mechanism.

(ii) The transition structures associated with these processes are highly asynchronous. The degree of advancement of the σ bonds being formed is sensitive to the method used in the optimization of the saddle point. A correlated method such as B3LYP predicts that the O1···C2 bond is more advanced than the C3···C4 bond.

(iii) The [$_\pi 2_s$ + ($_\pi 2_s$ + $_\pi 2_s$)] mechanism favors the formation of syn cycloadducts via transition structures whose geometry can be schematized as depicted in Figure 9. The origins of the stereoselection lie in the interaction between the endo substituent of the ketene and the chiral template. In the syn transition structure, this interaction is minimized and the large group is antiperiplanar to the C3···C4 bond being formed. In the anti transition structure, there is a destabilizing interaction between the endo substituent and the medium-size substituent of the carbonyl compound. The magnitude of these interactions is also controlled by the C3···C4 bond distance, which in turn is related to the nucleophilic or electrophilic character of the ketene. It is noteworthy that the geometries of these syn saddle points closely resemble the 1,3-allylic strain model proposed by Kishi[62,64] for the cis hydroxylation of chiral allylic ethers. Similarly, the anti saddle points are related to those proposed by Vedejs[63,64] for the same reaction.

(iv) In the lithium-assisted version of the reaction, the aldehyde and the lithium cation can form a chelated ion−molecule complex. The main features of this complex are kept in the corresponding transition structure, thus leading again to the preferential formation of the syn cycloadduct as schematized in Figure 9. The features of these transition structures are those expected from the cyclic Cram model, in which the ketene attacks the chelated lithium−aldehyde complex through its less hindered side.

(v) Calculations predict that thermodynamic control favors preferential formation of anti cycloadducts.

(62) Cha, J. K.; Christ, W. J.; Kishi, Y. *Tetrahedron* **1984**, *40*, 2247.
(63) Vedejs, E.; McClure, C. K. *J. Am. Chem. Soc.* **1986**, *108*, 1094.
(64) For a recent computational study on the stereochemistry of this reaction, see: Haller, J.; Strassner, T.; Houk, K. N. *J. Am. Chem. Soc.* **1997**, *119*, 8031.

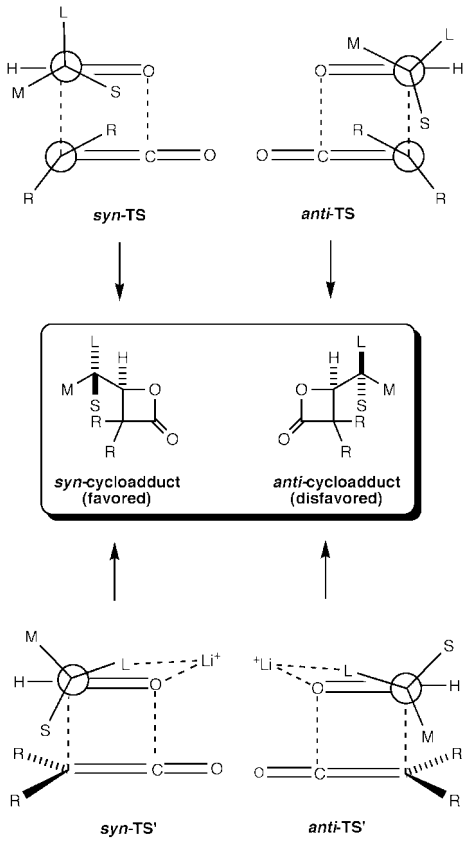

Figure 9. Schematic representation of the possible transition structures leading to the formation of *syn*- and *anti*-2-oxetanones. S, M, and L stand for the small, medium, and large substituents.

(vi) The predictions made on the basis of our computational studies have been verified experimentally. Reaction between (*S*)-2-(benzyloxy)propanal and dichloroketene, ketene, and dimethylketene leads to the corresponding *syn*-2-oxetanones with virtually complete stereocontrol. It is also found that the cycloaddition is facilitated when the reaction is carried out using 5 M LPDE as solvent.

(vii) The [2 + 2] cycloaddition between carbonyl compounds and ketenes can be considered as a pericyclic alternative to the nonchelation-controlled aldol reaction, with a complementary stereochemical outcome.

Experimental Section

General Methods. Commercially available compounds were used as such without further purification. Solvents were anhydrized and distilled according to standard protocols.[65] Diethyl ether was further dried and distilled over sodium−acetophenone. Lithium perchlorate, purchased from Aldrich (A.C.S. reagent), was dried at 160 °C and 0.05 mmHg with silica gel for 4 h in a Kügelrohr apparatus prior to use. We have found that this treatment is essential to carry out successful and reproducible experiments (CAUTION: perchlorates are potentially explosive compounds. Under the conditions described above, lithium perchlorate can be manipulated safely). Acyl chlorides[66] and (*S*)-(benzyloxy)propanal **2b**[67] were prepared by means of previously reported procedures. Flash chromatography purifications were performed using silica gel (230−400 mesh) and 1:20 AcOEt/hexanes mixtures.

The glassware used in the cycloaddition reactions was oven or flame dried and assembled under a slightly positive argon pressure. Melting points are uncorrected. Chemical shifts in the ^{1}H NMR spectra are reported as δ values (ppm) relative to internal tetramethylsilane (δ = 0.00 ppm). The NOE experiments were run at 300 MHz by preirradiating the desired signals for 15 s with the decoupler channel turned on at 15 db below 1 W and acquiring the spectrum with the decoupler turned off. The enhancements were directly measured by integration of the signals resulting from the respective difference spectra.

General Procedure for Cycloaddition Reactions in 5 M LPDE. Triethylamine (1.1 equiv) was added at 0 °C (ice−water bath) under argon atmosphere over a vigorously stirred solution of the corresponding acyl chloride (2 or 4 equiv, see the Supporting Information) and (*S*)-2-(benzyloxy)propanal **2b** (0.16 g, 1 mmol) in 2 mL of 5 M LPDE. After being stirred at room temperature or 0−5 °C for a certain time, the reaction mixture was diluted with dichloromethane (15 mL), and the resulting solution was washed successively with water, 1 N HCl, and a saturated solution of sodium bicarbonate. The organic layer was dried, the solvent was evaporated under reduced pressure, and the resulting residue was purified by flash chromatography or bulb-to-bulb distillation.

(*R*)-4-[(*S*)-1-(Benzyloxy)ethyl]-3,3-dimethyl-2-oxetanone (*syn*-3f) was obtained from isopropyl chloride (1 equiv) following the general procedure. The crude product was purified by flash chromatography as a colorless oil: yield 58%; $[\alpha]^{25}_D$ +26.0 (c = 0.4, CH_2Cl_2); IR (film) 1825 cm^{-1}; ^{1}H NMR ($CDCl_3$) δ 7.38−7.24 (m, 5H), 4.68 (d, 1H, J = 11.8 Hz), 4.64 (d, 1H, J = 11.8 Hz), 4.15 (d, 1H, J = 8.6 Hz), 3.74 (dq, 1H, J = 6.2 Hz, J' = 8.6 Hz), 1.42 (s, 3H), 1.28 (s, 3H), 1.19 (d, 3H, J = 6.2 Hz); ^{13}C NMR($CDCl_3$) δ 174.9, 138.1, 128.4, 127.6, 85.7, 73.4, 71.7, 22.8, 16.9, 16.4.

(*R*)-4-[(*S*)-1-(Benzyloxy)ethyl]-3,3-dimethyl-2-oxetanone (*anti*-3f). A cooled solution (0−5 °C) in THF (10 mL) of diisopropylamine (0.31 mL, 2.2 mmol) and a catalytic amount of 1,10 phenantroline was treated with a few drops of *n*-butyllithium until the solution had a dark red color. Then, a 1.6 M solution of *n*-butyllithium in hexanes (1.38 mL, 2.2 mmol) was added via syringe over 2 min. After 15 min, the resulting mixture was cooled to −78 °C, and 2-pyridyl isobutanethioate (0.36 g, 2 mmol) or phenyl isobutanethioate (0.36 g, 2 mmol) was added dropwise via syringe over 5 min. After 30 min, a solution of (*S*)-(benzyloxy)propanal (0.33 g, 2 mmol) in THF (5 mL) was added dropwise over 20 min via a cannula that was cooled at −78 °C (dry ice−acetone bath) by means of a glass tube with rubber septum. The reaction mixture was stirred at −78 °C for 30 min and at 0−5 °C for 75 min and then allowed to reach room temperature. Half-saturated NH_4Cl solution (10 mL) was then added, and the resulting mixture was partitioned between 15 mL of water and 15 mL of diethyl ether. The organic layer was washed with 10% K_2CO_3 solution (2 × 25 mL) and a saturated solution of NaCl (25 mL) and dried ($MgSO_4$), and the solvent was evaporated under reduced pressure to yield the crude product, which was purified by flash chromatography: yields 39% (with phenyl isobutanethioate) and 61% (with 2-pyridyl isobutanethioate). $[\alpha]^{25}_D$ +26.5 (c = 1.3, CH_2Cl_2); IR (film) 1825 cm^{-1}; ^{1}H NMR ($CDCl_3$) δ 7.36−7.26 (m, 5H), 4.66 (d, 1H, J = 11.2 Hz), 4.43 (d, 1H, J = 11.2 Hz), 4.02 (d, 1H, J = 8.7 Hz), 3.78 (dq, 1H, J = 8.7 Hz, J' = 6.0 Hz), 1.44 (s, 3H), 1.35 (d, 3H, J = 6.0 Hz), 1.32 (s, 3H); ^{13}C NMR ($CDCl_3$) δ 175.2, 137.6, 128.5, 127.9, 104.4, 83.3, 73.2, 70.6, 23.1, 16.7, 16.1.

General Procedure for the Conversion of 2-Oxetanones (3) into Butyrolactones. Titanium tetrachloride (1 M solution in CH_2Cl_2, 1 mL) was added over a solution of the corresponding 2-oxetanone **3** (1 mmol) in dichloromethane (2.5 mL). The reaction mixture was stirred for a certain time at different temperatures and was monitored by thin-layer chromatography. Water (7 mL) was added, and the resulting mixture was extracted with CH_2Cl_2 (3 × 7 mL). The organic layers were combined and filtered twice through a Celite pad.

(65) Perrin, D. D.; Armarego, W. L. F. *Purification of Laboratory Chemicals*; Pergamon: Oxford, 1988.
(66) Baumgarten, H. E.; Bower, F. A.; Okamoto, T. T. *J. Am. Chem. Soc.* **1957**, *79*, 3145.
(67) Zemribo, R.; Romo, D. *Tetrahedron Lett.* **1995**, *36*, 4159.

The filtrate was dried ($MgSO_4$), and the solvent was evaporated under reduced pressure. The resulting oily residue was purified by flash chromatography.

(4*S*,5*S*)-4-Hydroxy-3,3,5-trimethyl-2-oxolanone (*syn*-8) was prepared from ***syn*-3f** following the general procedure. The reaction was conducted at −78 °C for 30 min. The product was obtained as a colorless oil: yield 96%; $[\alpha]^{25}_D$ −56.0 (c = 0.62, CH_2Cl_2); IR (film) 1750 cm^{-1}; ^1H NMR ($CDCl_3$) δ 4.68 (dq, 1H, J = 3.7 Hz, J' = 6.5 Hz), 3.92 (d, 1H, J = 3.7 Hz), 2.2 (s_b, 1H), 1.26 (s, 6H), 1.42 (d, 3H, J = 6.5 Hz); ^{13}C NMR ($CDCl_3$) δ 181.6, 77.4, 77.2, 45.9, 22.8, 17.9, 13.8.

(4*R*,5*S*)-4-Hydroxy-3,3,5-trimethyl-2-oxolanone (*anti*-8) was prepared from ***anti*-3f** following the general procedure. The reaction was conducted at room temperature for 12 h. The product was obtained as colorless crystals: yield 79%; mp 70−71 °C (ethyl acetate−hexanes); $[\alpha]^{25}_D$ −46.0 (c = 0.1, CH_2Cl_2); IR (film) 1736 cm^{-1}; ^1H NMR ($CDCl_3$) δ 4.24 (dq, 1H, J = 6.2 Hz, J' = 7.9 Hz), 3.75 (dd, 1H, J = 5.9 Hz, J' = 7.9 Hz), 2.58 (d, 1H, J = 6.2 Hz), 1.47 (d, 3H, J = 6.2 Hz), 1.26 (s, 3H), 1.18 (s, 3H); ^{13}C NMR ($CDCl_3$) δ 180.2, 81.5, 78.0, 43.8, 22.7, 18.2, 17.6. Anal. Calcd for $C_7H_{12}O_3$: C, 59.30; H, 8.40; O, 33.29. Found: C, 59.35; H, 8.38; O, 33.31%.

(4*S*,5*S*)-4-(Benzyloxy)-5-methyl-2-oxolanone (6). Compound ***syn*-3d** was prepared from acetyl chloride (4 equiv) and **2b** following the general procedure (vide supra). The crude [2 + 2] cycloadduct was characterized by its spectroscopic features (see Figure 1 of the Supporting Information). Attempts to purify this cycloadduct failed, and so it was used as such in the following steps. Magnesium dibromide (3.3 g, 18 mmol) was added over a solution of crude ***syn*-3d** (9 mmol, theoretical from **2b**) in dichloromethane (18 mL). The resulting mixture was stirred for 30 min at room temperature, and then water (20 mL) was added. The aqueous layer was washed with dichloromethane (2 × 20 mL). The organic layers were combined and dried ($MgSO_4$), and the solvent was evaporated under reduced pressure. Purification by flash chromatography gave the title product as a colorless oil: yield 55% (overal from **2b**); $[\alpha]^{25}_D$ +26.2 (c = 1.04, CH_2Cl_2); IR (film) 1709 cm^{-1}; ^1H NMR ($CDCl_3$) δ 7.35−7.26 (m, 5H), 4.61 (d, 1H, J = 11.6 Hz), 4.54 (d, 1H, J = 11.6 Hz), 4.33 (ddd, 1H, J = 9.1 Hz, J' = 6.1 Hz, J'' = 4.5 Hz), 3.68 (q, 1H, J = 6.1 Hz), 3.16 (dd, 1H, J = 16.8 Hz, J' = 4.5 Hz), 2.87 (dd, 1H, J = 16.8 Hz, J' = 9.1 Hz), 1.33 (d, 3H, J = 6.1 Hz); ^{13}C NMR ($CDCl_3$) δ 176.6, 137.6, 128.4, 127.8, 76.9, 71.3, 51.1, 40.0, 17.2.

(+)-(*S*)-5-Methyloxol-3-en-2-one ((+)-(*S*)-β-Angelica Lactone 7). Titanium tetrachloride (1 M solution in dichloromethane, 1 mL) was added at room temperature over a solution of compound **6** (1 mmol) in dichloromethane (4 mL). The resulting mixture was stirred at the same temperature for 30 min. Water was then added, and the aqueous layer was extracted with dichloromethane (3 × 25 mL). The organic layers were combined and dried (Mg SO_4). Evaporation of the solvent gave an oily residue that was redissolved in dichloromethane (4 mL). Over this mixture, a solution of diisopropyl ethylamine (0.4 mL, 2.5 mmol) in dichloromethane (1 mL) was added at −20 °C. The resulting mixture was stirred for 5 h at −20 °C. Then, citric acid (10% solution, 20 mL) was added. The organic layer was separated and washed with $NaHCO_3$ (saturated solution, 20 mL) and water (20 mL). The organic layer was dried ($MgSO_4$), and evaporation of the solvent under reduced pressure gave an oily residue that was purified by distillation in a Kügelrohr apparatus: yield 42%; bp 100 °C/15 Torr (lit.[56a] bp 98−100/15 Torr); $[\alpha]^{25}_D$ +93.53 (c = 0.5, CH_2Cl_2) (lit.[56a] $[\alpha]^{25}_D$ +93.83 (c = 0.5, $CHCl_3$). The spectroscopic properties of the title compound were coincident with those previously reported.[56a]

Acknowledgment. The present work has been supported by the Secretaría de Estado de Universidades, Investigación y Desarrollo (Project PB96-1481), and by Gobierno Vasco/Eusko Jaurlaritza (Project GV 170.215-EX97/11). A grant from the Gobierno Vasco/Eusko Jaurlaritza to I.A. is gratefully acknowledged. We also thank the Plan Nacional de I+D (CICYT) and the CIEMAT for a generous gift of computing time at the Cray YMP-EL supercomputer.

Supporting Information Available: Additional experimental details and characterization of compounds *syn*-**3b**, **4**, and **5**; ^1H NMR and ^{13}C NMR spectra of all products described in the text; tables including Cartesian coordinates, total energies, and zero-point vibrational energies of all the transition structures and cycloadducts reported in this paper (37 pages). This material is contained in libraries on microfiche, immediately follows this article in the microfilm version of the journal, and can be ordered from the ACS; see any current masthead page for ordering information.

JO9806512